

INFN-14-10/GE
5th May 2014

Direct measurement of antares detector angular resolution with moon shadow effect

Matteo Sanguineti¹, Carla Distefano², Vladimir Kulikovskiy³, Heide Costantini⁴,
Christophe Hugon³.

¹*Università degli Studi di Genova, Dipartimento di Fisica and INFN – Sezione di Genova, Genova, Italy*

²*INFN – Laboratori Nazionali del Sud (LNS), Catania, Italy*

³*INFN – Sezione di Genova, Genova, Italy*

⁴*CPPM, Aix-Marseille Université, CNRS/IN2P3, Marseille, France*

Abstract

The cosmic ray Moon shadow analysis is a unique method to test the pointing performance of a neutrino telescope, like the ANTARES detector. In this article the 2007-2012 data sample is analysed and a 3.06σ significance of Moon shadow effect is found. For this analysis a dedicated Monte Carlo simulation has been produced and an opportune test statistic function has been defined. This is the first direct measurement of the angular resolution of the ANTARES detector ($0.7^\circ \pm 0.2^\circ$).

1 INTRODUCTION

The ANTARES detector is the biggest neutrino telescope in the Northern hemisphere. It is installed 40 km offshore from Toulon (France) at a depth of 2475 m. The detector is constituted by twelve vertical lines (350 m long), there are 75 PMTs on each line installed for the detection of Cherenkov light induced by muons¹. The detector was completed in May 2008.

In this kind of detectors the measure of the angular resolution and the absolute pointing accuracy is really critical. The pointing performance of the detector depends on the relative delays of the optical sensors within each detector line as well as between the lines, but also on the instantaneous shape and absolute orientation of the detector lines.

The relative time delays have been evaluated using laser and LED beacons, whereas the alignment is monitored with acoustic emitters and transceivers, tiltmetres and compasses. Finally the absolute orientation is provided by the triangulation of acoustic signals between lines and the deployment vessel at the sea surface using GPS.

Due to the complexity of all these operations, it may be helpful to verify the performance of the detector using a calibration source. The simplest solution is the measurement of the so-called “Moon Shadow” effect. The interaction of cosmic rays in the atmosphere produces down-going muons that are detected by the ANTARES telescope. However the Moon absorbs the cosmic rays, so the detector will see a deficit in the events density corresponding to the direction of the Moon disk (Fig. 1).

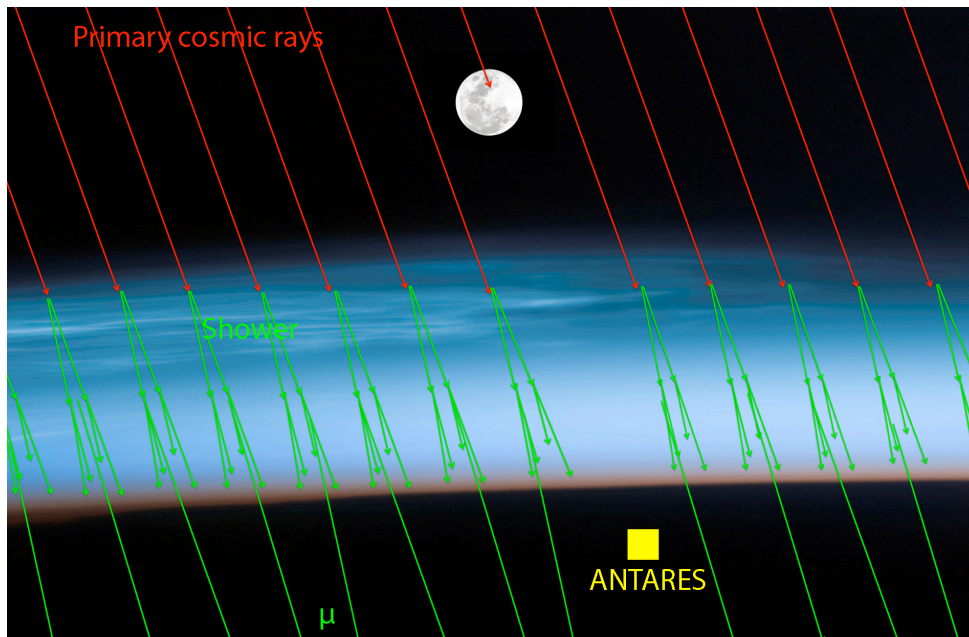


FIG. 1: Primary cosmic rays absorption would cause a secondary muons deficit in the ANTARES detector.

The Moon shadow effect has been used also by the ICECUBE collaboration to test the pointing performance of the detector².

A similar analysis was carried out for our detector: the used data set corresponds to the period 2007-2012 and the same track reconstruction algorithm as for the point source search was used³⁾.

2 MOON SHADOW SIMULATION

The simulation of the Moon shadow effect is based on the version 2 of the standard ANTARES Run by Run Monte Carlo⁴⁾. The ANTARES run by run simulation includes present environmental conditions as well as present detector configuration. It simulates muon events on full sky with a weight of 10; in fact a simulation of each muon will require too much CPU time, so only one muon over 10 is simulated.

However muons coming around the Moon disk are really important in this analysis, so a new dedicated production of Monte Carlo has been made, where muons coming in a disk of 10° around the Moon centre have a weight of 1 (the Moon disk has a radius of 0.259°).

Also muons coming outside the 10° disk will be taken in account using the standard Monte Carlo production with weight equal to 10.

In this analysis two different Monte Carlo simulation were performed: one supposing a shadowing effect of the cosmic rays, the other without this event suppression.

The two simulations correspond to the data period of 2080 days considered in this analysis.

The simulation takes in account the geomagnetic deflection of the cosmic rays.

First the deflection of cosmic rays in the path from the Moon to the Earth atmosphere is taken in account analytically. The obtained deflection is then supplied as input to the Monte Carlo simulation. The deflection of 10 TeV protons is shown in Fig. 2 as a function of the Earth distance.

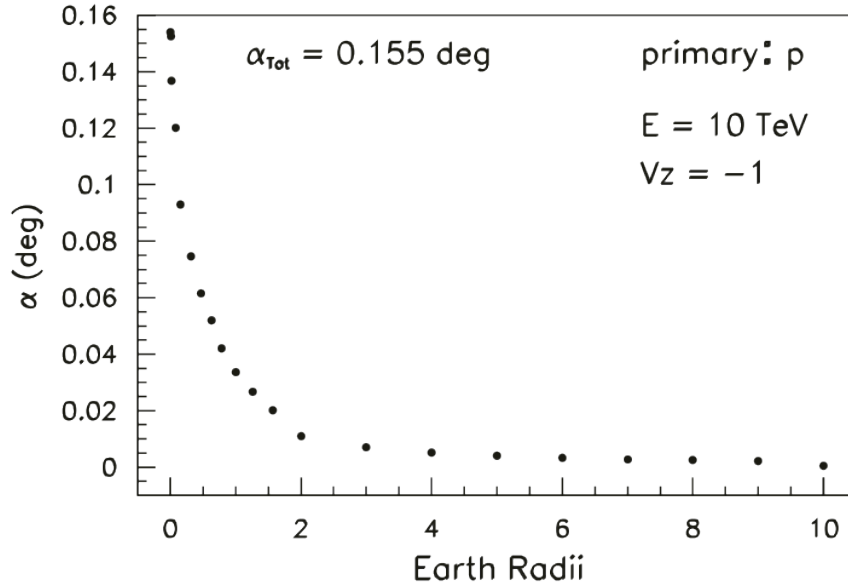


FIG. 2: Angular deviation integrated over the path length in units of Earth radii. Calculation has been carried out for a proton with energy $E = 10$ TeV and perfectly vertical.

Then the deflection of atmospheric muons is included in the Monte Carlo simulation and the result are shown in Fig. 3

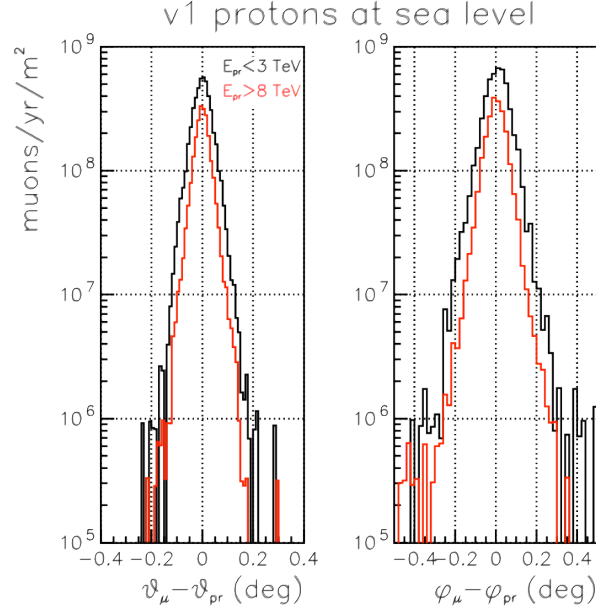


FIG. 3: Zenithal (θ) and azimuthal (ϕ) deflection at sea level of atmospheric muons. Black curve: muon with energy lower then 3 TeV; red curve: muon with energy higher then 8 TeV.

The overall deflection at sea level and at detector level is shown in Fig. 4.

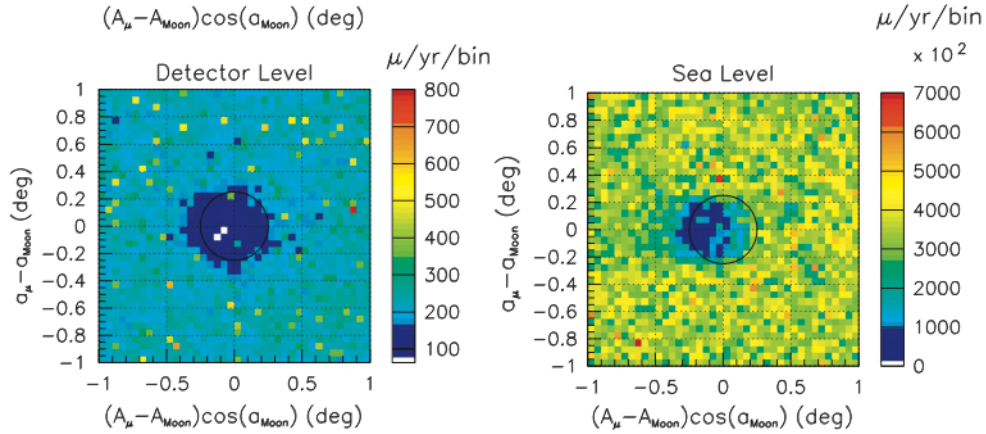


FIG. 4: Atmospheric muons coming from the Moon region and reaching the sea level (right) and the detector (left). Maps are plotted in Moon relative horizontal coordinates. The black circle represents the Moon disk.

A deflection is clear at sea level. However it is completely negligible at detector level because the highly deflected muons have low energy and they are absorbed before reaching the detector.

The region around the Moon centre is divided in many concentric ring with increasing radius. The events density of each ring n is defined as the number of events detected in that sector over the surface of the ring.

Then a method to evaluate the statistical significance has been developed for this measure.

A test statistic function t is defined as:

$$t = \sum_{ring} \left(\frac{(n_m - n_{exp, NO Moon})^2}{n_{exp, NO Moon}} - \frac{(n_m - n_{exp, Moon})^2}{n_{exp, Moon}} \right)$$

where the sum is over all the ring around the Moon centre; n_m is the density of events measured in a ring, $n_{exp, Moon}$ is the expected density of the ring in “Moon shadow” hypothesis and $n_{exp, NO MOON}$ is the expected density of the ring in “no Moon shadow” hypothesis.

Many toy simulation were generated in order to obtain the distribution of the variable t in the case of Moon shadow effect or vice versa (Fig. 5).

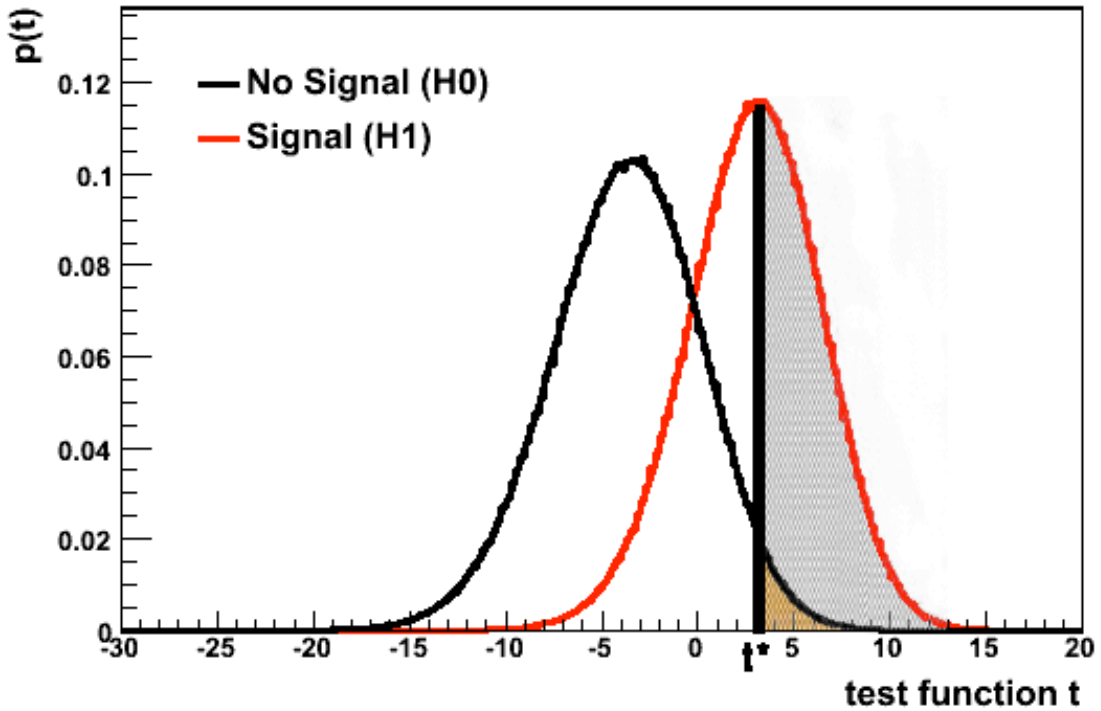


FIG. 5: An example of the test function t distribution in “Moon shadow” hypothesis (red curve) and “no Moon shadow” hypothesis (black curve). The shaded area is the fraction of the toy experiments where the Moon shadow hypothesis will be correctly identified as evidence of the shadowing effect, then the orange area is the significance.

The shaded area shows the fraction of the toy experiments where the Moon shadow hypothesis will be correctly identified as evidence of the shadowing effect; this fraction was fixed to 50%. The value of t corresponding to this fraction of the “Moon shadow” toy experiments will be called t^* , in other words it is the reference value of the test statistic.

The orange area in Fig. 5 shows the minimum significance of the Moon shadow discovery for experiments with t above t^* . This area also corresponds to the fraction of “no Moon shadow” toy experiments that will be wrongly identified as the evidence of shadowing effect. In the next section the optimisation of the selection criteria on reconstructed tracks in order to maximize this significance level will be presented. After the optimization, when the real measurement is done and the measured value of t is calculated, the actual significance can be evaluated.

3 OPTIMIZATION OF SELECTION CRITERIA ON RECONSTRUCTED TRACK

An accurate study on selection criteria of reconstructed tracks was performed. Some parameters characterize the tracks achieved by the usual reconstruction algorithm of the ANTARES collaboration³⁾: the angular error of the direction β , the quality of the reconstructed track Λ and the number of hits used in the reconstruction.

Exploiting the method described in the previous paragraph, the significance of the measure was estimated using different selection criteria on events.

First, the quality of the reconstructed track Λ was analysed. Fig. 6 shows the expected significance (expressed as number of σ) as a function of Λ , i.e. including only events with Λ greater then a determinate value (dedicated 10° around the Moon simulation and RbR simulation outside the disk).

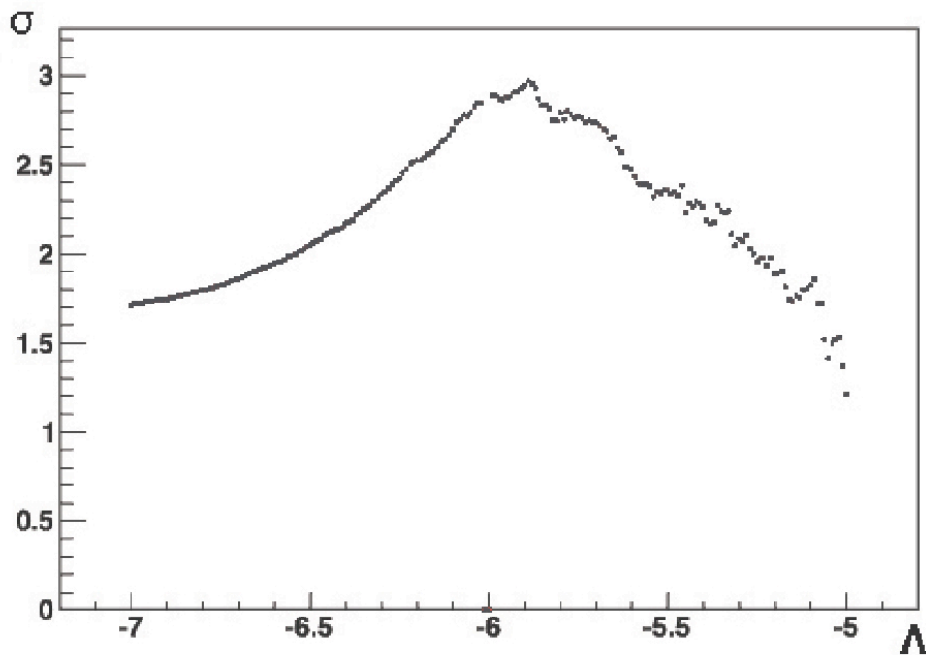


FIG. 6: Expected significance (expressed as number of σ) as a function of Λ .

For value of Λ between -6 and -5.9 the significance is almost 3σ .

Typically in the ANTARES collaboration analysis, the parameter Λ provides the most considerable and effective selection on events, but sometimes other parameters can be useful in the selection.

In order to evaluate the efficiency of the cuts, the expected significance will be shown as a function of Λ and of one of these parameters.

For instance, in Fig. 7 the expected significance as a function of Λ is shown for tracks with an angular error β less than a determinate value.

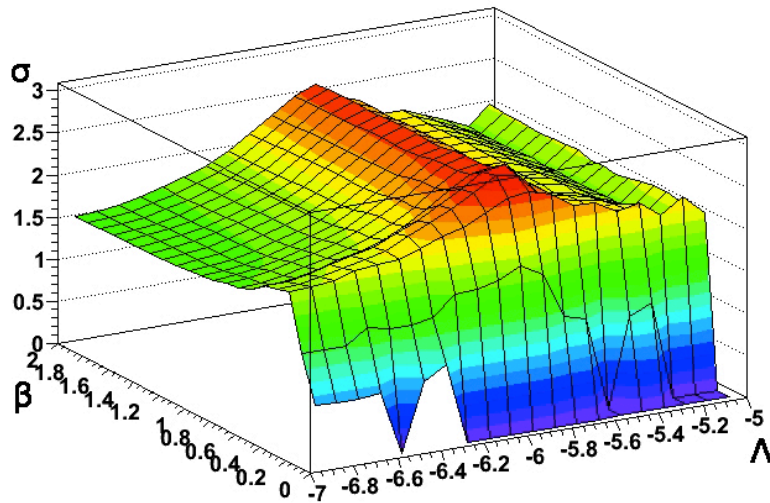


FIG. 7: Expected significance (expressed as number of σ) as a function of Λ and β .

It is clear that the significance depends definitely more on Λ than on β . Anyway the best selection criteria on the angular error is $\beta < 0.8^\circ$.

In Fig. 8 and Fig. 9 is shown the expected significance as a function of Λ and the number of hits used in the track reconstruction.

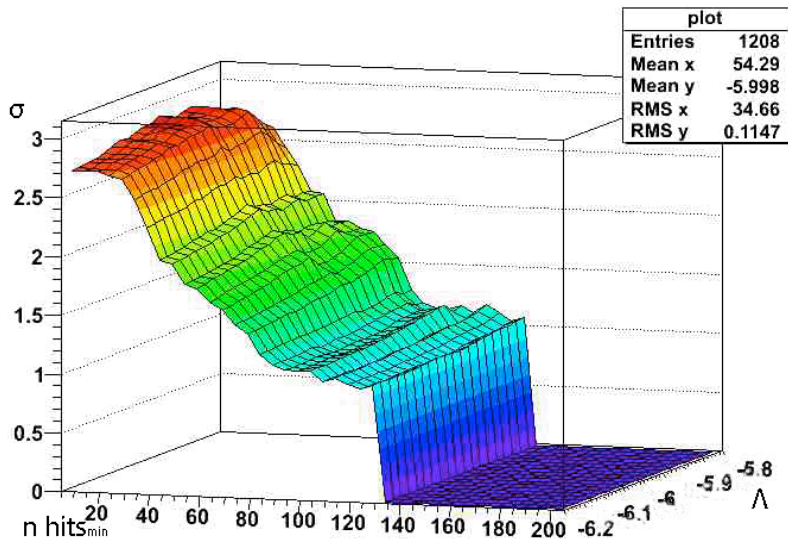


FIG. 8: Expected significance (expressed as number of σ) as a function of minimum number of hits and Λ .

In the first plot are shown only events that have number of hits greater than a determinate value, in this way tracks with few hits are eliminated (this tracks have substantial uncertainty).

The figure proves that the expected significance increases while the minimum number of hits decrease, so this selection seems to be useless for this analysis.

Likewise it was checked if a selection on the maximum number of hits could be useful, in this way the multi-muon events could be rejected (Fig. 9).

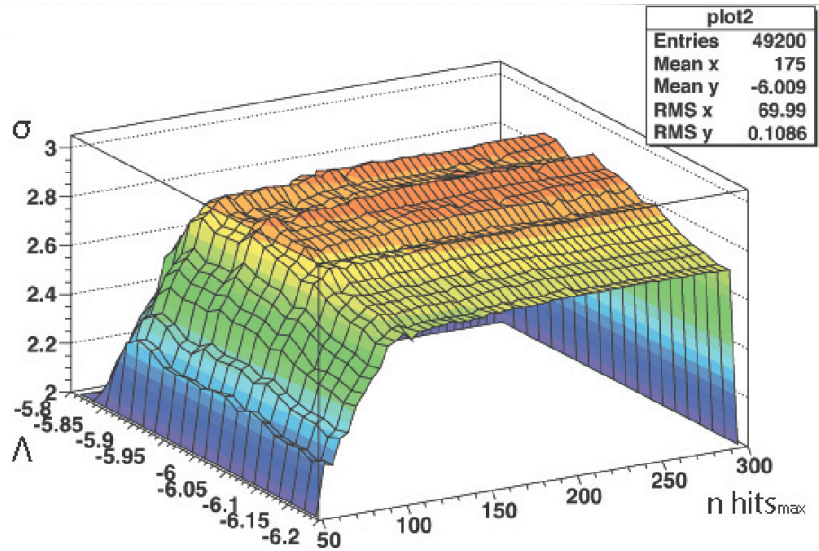


FIG. 9: Expected significance (expressed as number of σ) as a function of maximum number of hits and Λ .

Also this time the dependence is really weak and the greater significance is obtained for higher value of maximum number of hits, so also this selection is not useful for the analysis.

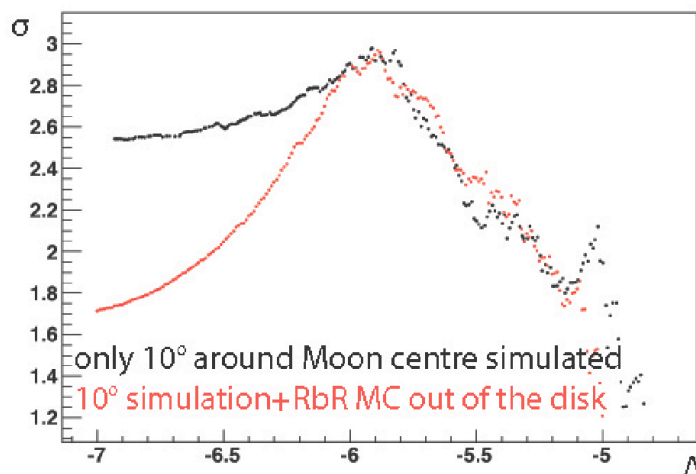


FIG. 10: Expected significance (expressed as number of σ) as a function of Λ . Red point: using only dedicated simulation. Black point: dedicated simulation and RbR Monte Carlo outside the 10° disk.

Now will be presented a comparison between the result of the simulations using only tracks coming inside the 10° radius disk around the Moon centre or the full sky simulation.

Fig. 10 shows the significance as a function of Λ .

It is clear that using only the dedicated simulation the significance for poorer value of Λ is overestimated, but in any case for value of Λ between -6 and -5.9 the significance is almost 3σ .

As further evidence, in Fig. 11 is shown the significance as a function of β for tracks with $\Lambda > -5.9$.

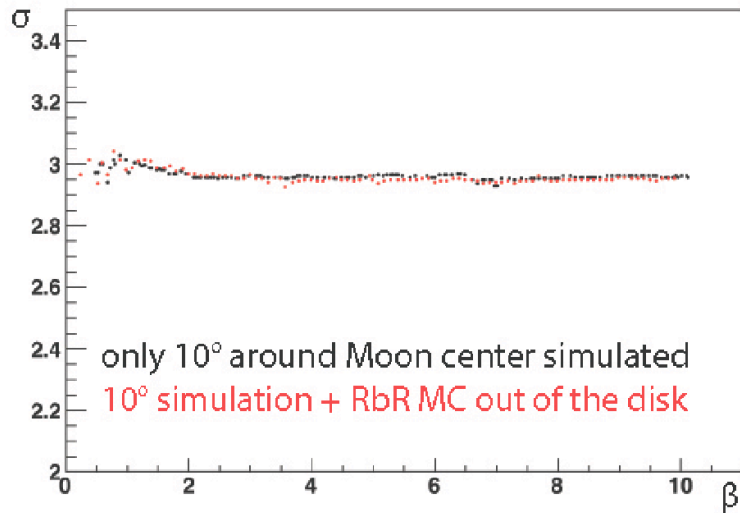


FIG. 11: Expected significance (expressed as number of σ) as a function of β for tracks with $\Lambda > -5.95$. Red point: using only dedicated simulation. Black point: dedicated simulation and RbR Monte Carlo outside the 10° disk.

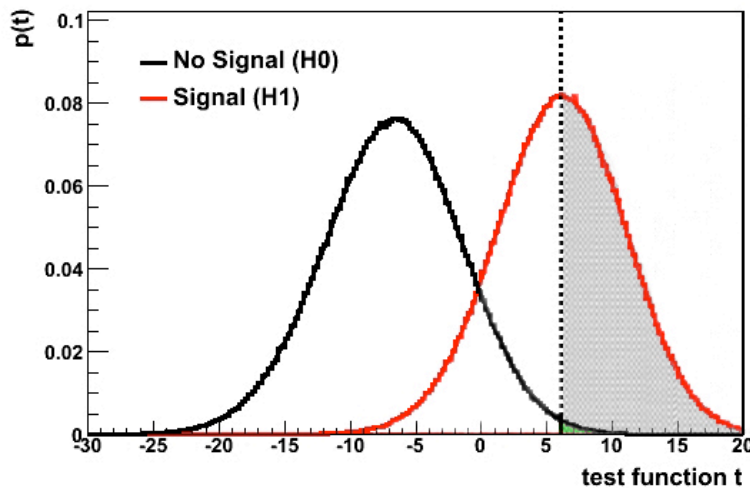


FIG. 12: Test function t distribution in “Moon shadow” hypothesis (red curve) and “no Moon shadow” hypothesis (black curve) according to the optimized selection criteria ($\Lambda > -5.9$ and $\beta < 0.8$). The shaded area is the fraction of the toy experiments where the Moon shadow hypothesis will be correctly identified as evidence of the shadowing effect, then the green area is the significance.

The two simulation are quite compatible, so the tracks outside the 10° disk do not affect much the result of the simulation, if a proper cut on Λ is used.

According to the result of the simulation, the selection criteria chosen are $\Lambda > -5.9$ and $\beta < 0.8$. and the corresponding test statistic function distribution is shown in Fig. 12.

The expected significance is 2.9σ and the reference value of the test statistic t is 6.15.

4 DATA ANALYSIS

The results of the comparison between the data and the Monte Carlo (Moon shadow and No Moon shadow hypothesis) are shown in Fig. 13.

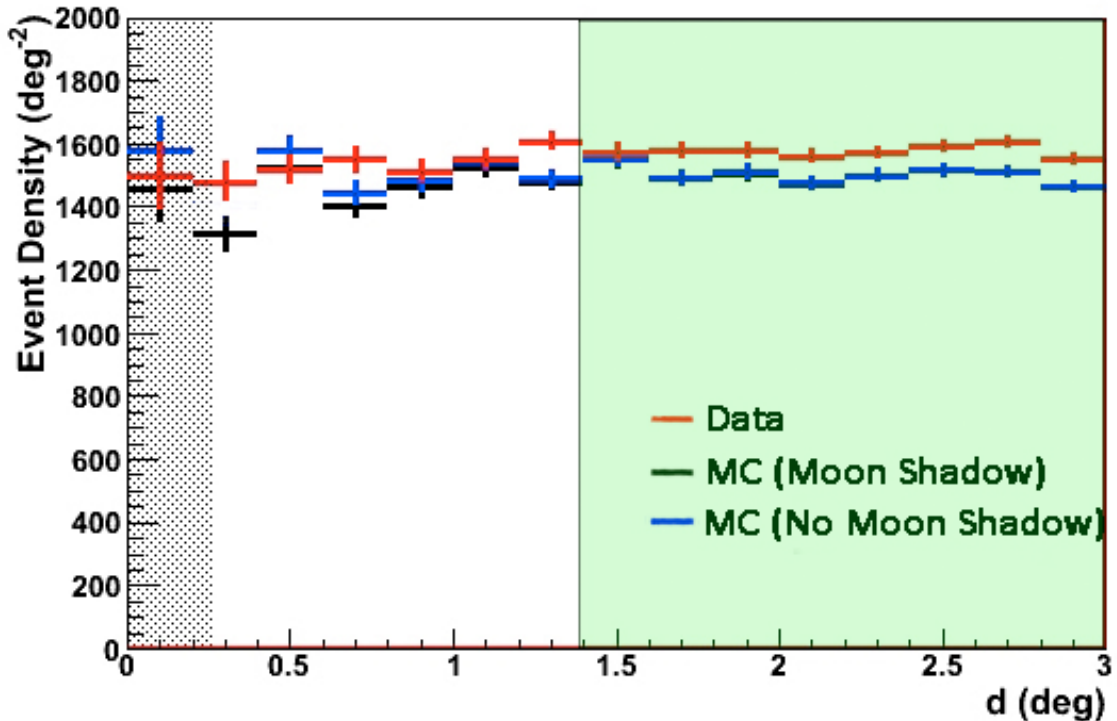


FIG. 13: Muons events density in different rings around the Moon centre as a function of the angular distance of the ring. The region considered for the renormalization of the MC is coloured in green.

A 6% discrepancy between data and Monte Carlo is found in the region where the Moon shadowing effect is expected to be negligible.

This kind of discrepancy was found in similar muons ANTARES analysis and corresponds to systematic uncertainties due to the primary flux and detector configuration, so the Monte Carlo was renormalized according to the number of events simulated in the green region of Fig. 13, where the two different Monte Carlo are perfectly identical.

The results after renormalization are shown in Fig. 14.

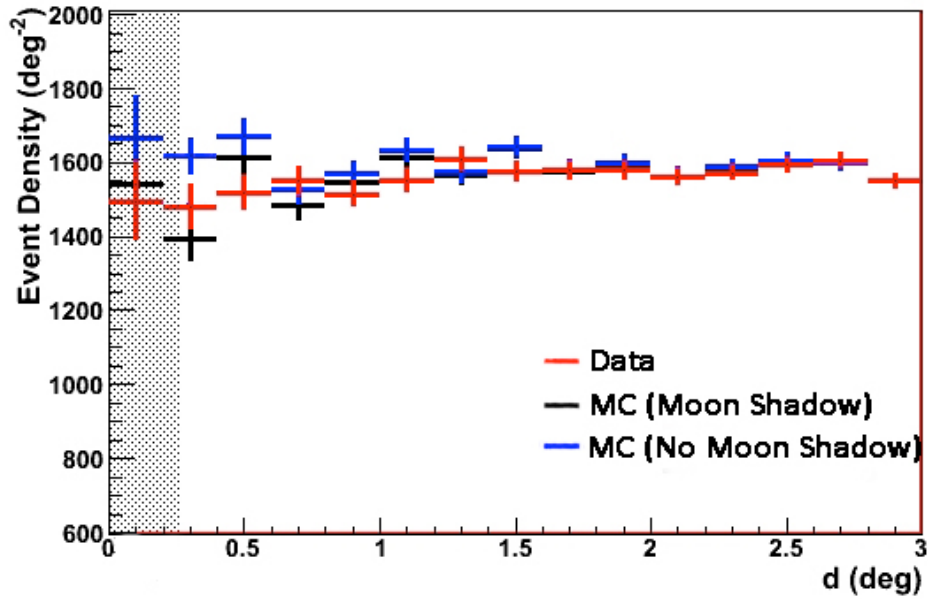


FIG. 14: Muons events density in different ring around the Moon centre as a function of the angular distance of the ring after renormalization of the Monte Carlo.

The data/MC(Moon Shadow) ratio is presented in Fig. 15.

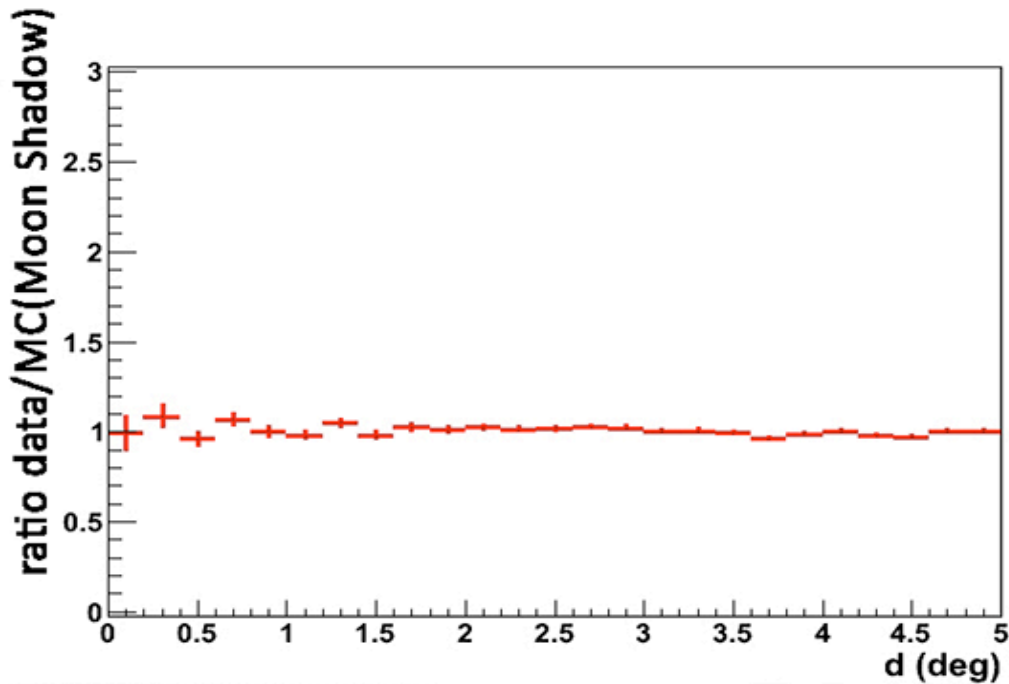


FIG. 15: Ratio data/MC(Moon Shadow).

The ratio is compatible with 1 in all the angular range around the Moon.

In this data analysis the value of the test statistic function t is 7.12, so the “No Moon shadow” can be rejected with a significance of 3.06σ . In Fig. 16 the muon density around the Moon centre is shown with a Gaussian fit of the deficit.

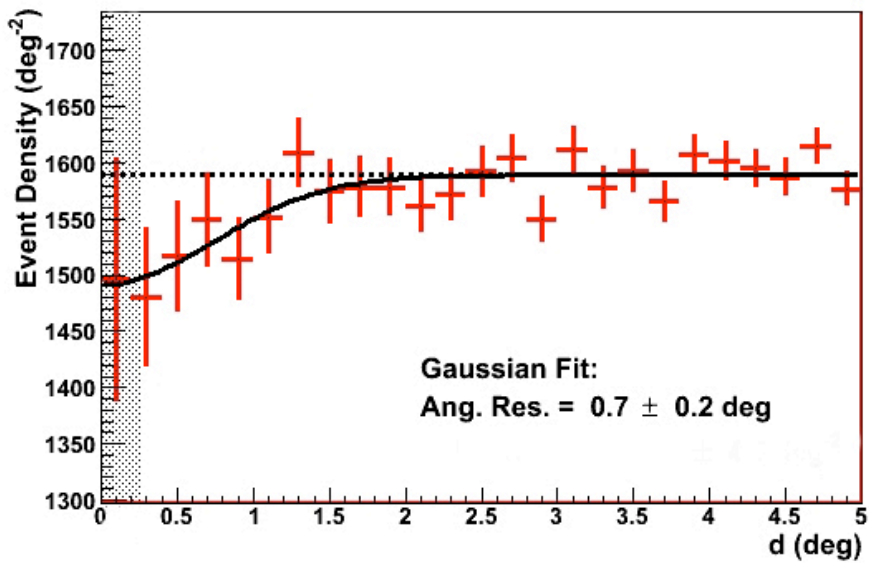


FIG. 16: Gaussian fit of the muon events density.

In Fig. 17 similar Gaussian fit are also shown for the two MC.

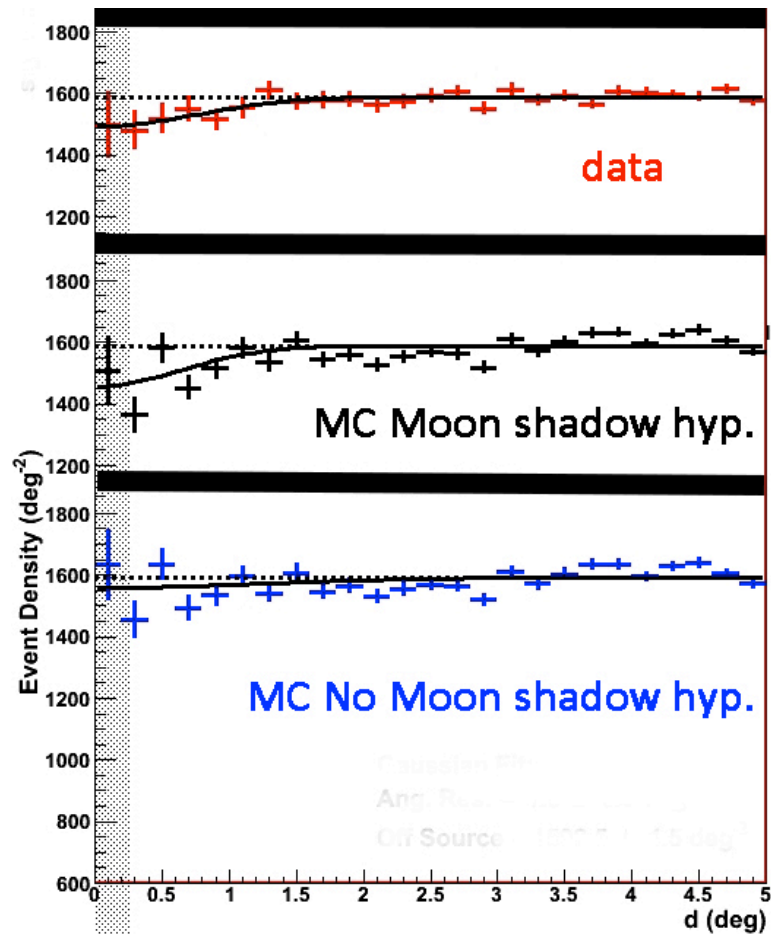


FIG. 17: Comparison of the Gaussian fit of data, MC (Moon shadow) and MC (No Moon shadow).

The measurement of the angular resolution from the Gaussian fit is $0.7^\circ \pm 0.2^\circ$. In Fig. 17 similar Gaussian fit are also shown for the two MC.

The angular resolution of the MC (Moon shadow) is $0.6^\circ \pm 0.1^\circ$ in good agreement with the result of the data analysis.

5 CONCLUSIONS

In this paper the Moon shadow effect has been used to test the pointing performance of the ANTARES detector. A dedicated Monte Carlo simulation and an opportune test statistic function has been developed to evaluate the best selection criteria for the analysis.

The 2007-2012 data sample show a 3.06σ evidence of Moon shadow effect and the corresponding measured angular resolution of the detector is $0.7^\circ \pm 0.2^\circ$. This is the first MC independent measurement of the angular resolution of the ANTARES detector.

6 REFERENCES

- (1) ANTARES collaboration, ANTARES: the first undersea neutrino telescope. Nuclear Instruments & Methods in Physics Research Section A (2011)
- (2) ICECUBE collaboration, Observation of the cosmic-ray shadow of the Moon with IceCube. arXiv:1305.6811 (2013)
- (3) A. Heijboer, An algorithm for track reconstruction in ANTARES. ANTARES-SOFT-2002-002 (2002)
- (4) C. Rivière, Run-by-run Monte Carlo simulation for ANTARES: v2. ANTARES-PHYS-2012-001 (2012)

7 REFERENCES

- (1) ANTARES collaboration, ANTARES: the first undersea neutrino telescope, arXiv:1104.1607.
- (2) A. Heijboer, Track reconstruction and point source searches with ANTARES, ANTARES-06-08-2004.
- (3) Jürgen Brunner, The BBfit Reconstruction algorithm, ANTARES-SOFT-2009-003.
- (4) Laura Core, private comm.